

Vortex-Induced Vibration of a Transversely Rotating Sphere

A. Sareen¹, J. Zhao¹, D. Lo Jacono², J. Sheridan¹, K. Hourigan¹, M. C. Thompson¹

¹Department of Mechanical and Aerospace Engineering
Monash University, Clayton 3800, Australia

²Département de Mécanique
Institut de Mécanique des Fluides Toulouse (IMFT)
Université de Paul Sabatier, Toulouse 31500, France

Abstract

Vortex-induced vibration (VIV) of a sphere is one of the most basic fluid-structure interaction problems. Since such vibrations can lead to fatal structural failures, numerous studies have focused on suppressing such flow-induced vibrations. In this study, for the first time, the effect of an imposed transverse rotation on the dynamics of the VIV of an elastically mounted sphere has been investigated. It was observed that the non-dimensional vibration amplitude for a rotating sphere ($A^* = \sqrt{2}y_{rms}/D$, where y_{rms} is the root mean square of the displacement in the transverse direction and $D =$ sphere diameter) exhibits a bell-shaped evolution as a function of reduced velocity, similar to the classic VIV response of a non-rotating sphere. The sphere is found to oscillate freely up to a rotation ratio α (ratio of the equatorial velocity of the sphere to the free-stream velocity) close to 0.5. For lower rotation ratios ($\alpha \leq 0.3$), the response looks similar to the non-rotating case but with slightly smaller vibration amplitude. For higher α values, the amplitude was found to decrease significantly with the rotation up to $\alpha = 0.5$. The amplitude dropped drastically after it reached the peak amplitude. This is unlike the VIV response of a rotating circular cylinder where the vibration amplitude increases up to three times the maximum vibration amplitude in the non-rotating case due to a novel asymmetric wake pattern (see [1]).

Introduction

Vortex-induced vibration (VIV) of structures can occur in a variety of engineering situations, such as bridges, transmission lines, offshore structures, heat exchangers, tethered structures, pipelines, and other hydrodynamic and hydroacoustic applications. This led to several comprehensive studies on VIV in the past (see [8] and [6]). Since such vibrations impact on the fatigue life of structures, they can lead to structural failures and are an important source of fatigue damage of offshore oil exploration and production risers. Numerous studies have focused on suppressing such flow-induced vibrations, especially for cylinders. However, there are no such studies for basic symmetrical three-dimensional bodies like spheres. In spite of its ubiquitous practical significance, there are few studies on the VIV response of a sphere and its suppression. The question that arises is, how can the VIV of such a simple 3D geometry be suppressed?

Previous numerical studies on the effect of rotation on rigidly mounted rotating spheres at low Reynolds numbers ($Re \leq 300$) ([7], [4]) revealed suppression of the vortex shedding for a certain range of spin ratios. So can the structural vibrations of a sphere be suppressed by an imposed rotation once the sphere is free to oscillate? The previous investigations on the VIV of spheres by [2] and [3], revealed that the sphere exhibits two modes of vibration, namely, mode I and mode II when the oscillation frequency is of the order of the static body vortex shedding. They showed that the vortex phase ϕ_v (phase difference between the vortex force and the body displacement) gradually

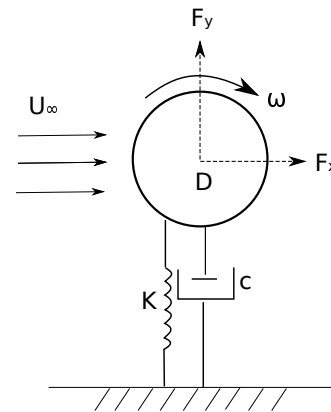


Figure 1: Definition sketch for the cross-flow VIV of a rotating sphere (Top view). The sphere undergoes free vibrations in the transverse direction to the free-stream U_∞ in the x-direction. The sphere rotates in the clockwise direction with rotational rate ω . Here k is the spring constant, and c is the damping of the system.

changes from ~ 50 degrees to ~ 150 degrees from mode I to mode II. But it is still unknown, how the vibration response of the sphere changes when a transverse rotation is imposed.

This is the first study reporting the effect of an imposed transverse rotation on the VIV response of a sphere. In the current study, an elastically mounted sphere free to oscillate in the transverse direction is considered over a wide range of parameter space of reduced velocities and rotational rates. The Reynolds number (based on sphere diameter and flow velocity) for the current study varies from 5000 to 30,000.

In this study, we seek to understand the following fundamental questions: How does the imposed transverse rotation affect the VIV response of the sphere? Does it suppress the vortex shedding at this high Reynolds number? Does the sphere continue to vibrate in the absence of vortex shedding?

In the first section, we will elaborate on the experimental methods used in the current study followed by a section on Results and Discussions in which, the findings from the current study are presented and discussed in detail.

Experimental Details

The experiments were conducted in the recirculating free-surface water channel of the Fluids Laboratory for Aeronautical and Industrial Research (FLAIR), Monash University, Australia. The test section of the water channel has dimensions of 600mm in width, 800mm in depth, and 400mm in length. The free-stream velocity in the present experiments was varied continuously in a range of $0.05 \leq U \leq 0.45$ m/s, corresponding to the pump frequency range of 5 – 50Hz. The free-stream turbulence levels were less than 1% for the current experiments.

Mass ratio	m^*	$m/(\pi\rho D^3/6)$
Amplitude ratios	A_y^*, A_x^*	$A_x/D, A_y/D$
Normalised velocity	U^*	$U/(f_n D)$
Scaled normalised velocity	U_s^*	$(U^*/f^*)S$
Reynolds number	Re	UD/μ
Strouhal number	S	$f_{vo}D/U$
Transverse frequency ratio	f^*	f/f_n
Damping ratio	ζ	$c/2\sqrt{k(m+m_A)}$
Rotation ratio	α	$D\omega/2U$

Table 1: Non-dimensional parameters. The added mass m_A , is given by $m_A = C_A m_d$, where m_d is the displaced fluid mass and C_A is the added mass coefficient (0.5 for a sphere). In the above parameters, f_n is the natural frequency of the system, D = sphere diameter, k = spring constant, ρ = fluid density, U = free stream velocity, μ = viscosity, m = total oscillating mass, c = structural damping, ω = rotational speed of the sphere, f_{vo} = non-oscillating body vortex shedding frequency, f = oscillation frequency, and A_x, A_y are the oscillation amplitudes in x and y directions respectively.

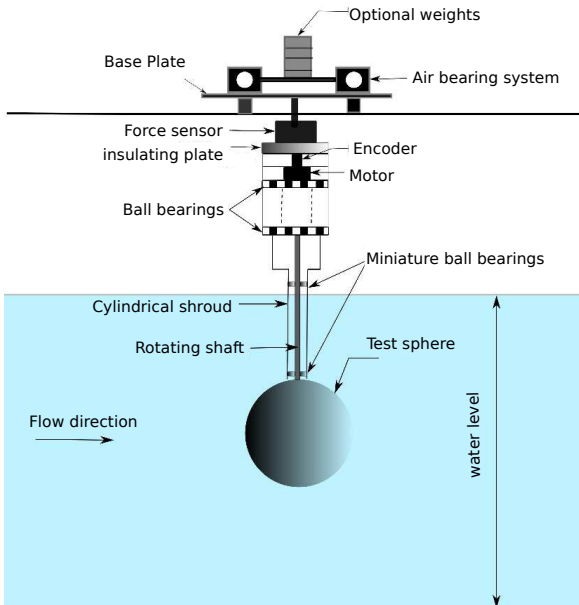


Figure 2: Schematic of the experimental setup used for the current study.

The schematic for the experimental setup is shown in figure 2. An air-bearing system with a low damping ratio was used to provide low-friction motion in the transverse direction. More details of the hydroelastic facility can be found in [9]. The body displacement was measured using a non-contact (magnetostrictive) linear variable differential transformer (LVDT). The fluctuating lift and drag forces were measured by a six-axis force sensor (ATI mini40/IP68), which was attached at the upper end of the rig. The sphere was driven at various rotational speeds using a miniature low-voltage LV172 Parker stepper motor. For each data set, the raw analog voltages were

acquired at 100Hz for 300 seconds at each flow velocity, and were converted to digital signals using a differential DAQ board system. The data sampling and recording were controlled via customised LabVIEW 8.5 VI programs, while the data processing and analysis were performed using MATLAB codes.

The spherical model used in the present study was a precision solid ball of diameter 80mm manufactured from acrylic plastic. The diameter of the supporting rod was approximately 27 times smaller than the sphere. The rotating driving shaft was covered with a non-rotating cylindrical shroud 6.35mm in diameter so as to avoid any interference from the rotating shaft. The top surface of the sphere was one diameter away from the free-surface in order to avoid any free surface effects. [5] reported that the free surface effect only kicks in when the immersed length is less than 0.5 times the sphere diameter for a tethered sphere. Free decay tests in water and air were performed to obtain the natural frequency and damping ratio of the system before each series of experiments.

Results and Discussions

Validation experiment: VIV of a non-rotating sphere

Figure 3 shows the classic one-degree of freedom vibration response of a sphere compared to the one reported by [2]. The mass ratio and the damping ratio for the current experiment were 7.8 and 0.004 compared to 7 and 0.004, respectively, by [2]. In figure 3, the non-dimensional amplitude of oscillations (defined as $A^* = \sqrt{2}A_{rms}/D$) is plotted against the scaled U^* , which is defined as $U_s^* = (U^*/f^*)S$, where S is the Strouhal number for the sphere. The lock-in starts at $U^* = 4 - 5$ for the sphere, which corresponds to a U_s^* of 0.7 – 0.875.

It can be noted that the vibration response gradually progresses to mode II from mode I, as opposed to the case of cylinders, where a sudden jump is observed between the vibration branches. In the case of cylinders, the sudden jump in ampli-

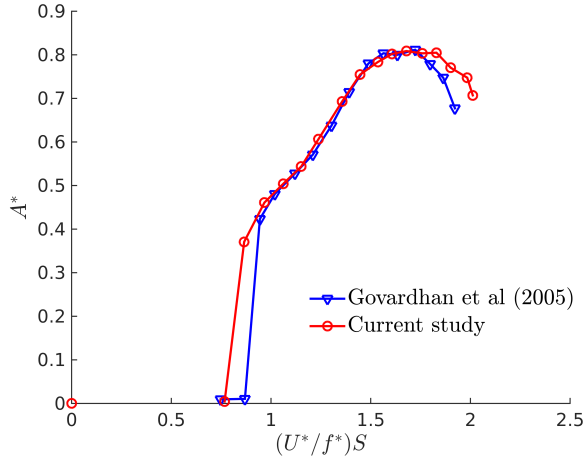


Figure 3: Comparison of the amplitude response obtained in the current study to that of Govardhan et al (2005). The mass ratio for the current study is 7.8 compared to a mass ratio of 7 in their study. The damping ratio was same in both the studies ($\zeta = 0.004$).

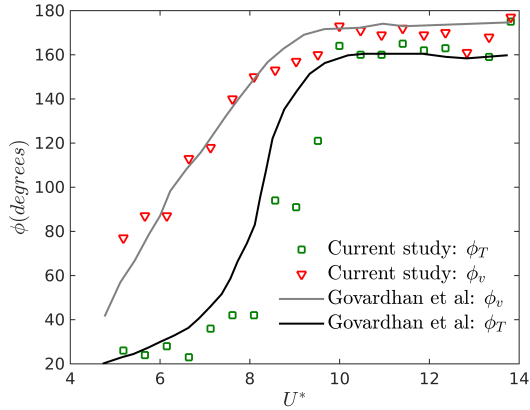


Figure 4: The variation of the total and vortex phase with the reduced velocity compared to the data by [2]. The mass ratio for the current experiment was 12 compared to 31.1 in their study.

tudes is associated with a sudden jump in the total phase difference (phase difference between the total fluid force in the transverse direction to the body displacement). However, in spheres, the vortex phase gradually changes from ~ 50 degrees to ~ 160 degrees, as shown in figure 4. Figure 4 shows the variation of the total and vortex phase difference with the reduced velocity in comparison to the ones reported by [2] for somewhat different experimental conditions.

For a very light tethered body, a desynchronised region can be observed between the two modes [2]. For elastically mounted bodies of higher mass, the transition is evident only as a dip in the amplitude response. Figure 5 shows the variation of the non-dimensional frequency $f^* = f/f_n$ (the ratio of the dominant oscillation frequency to the natural frequency in the water) with the reduced velocity. During lock-in ($U^* \sim 4$), the oscillation frequency stays close to the natural frequency of the system.

VIV of a rotating sphere

A non-dimensional rotation ratio α is the main parameter

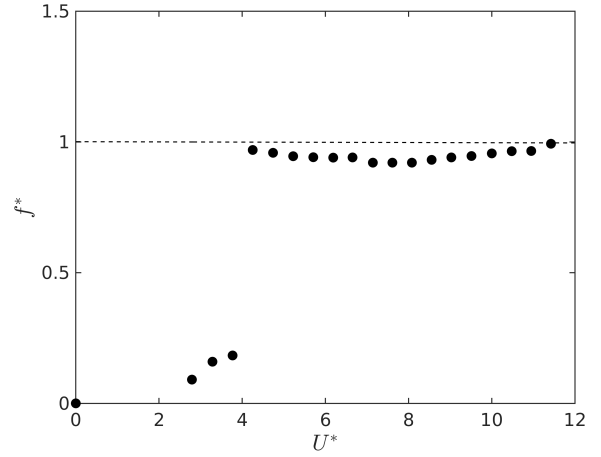


Figure 5: The frequency response corresponding to the same experimental conditions as figure 3.

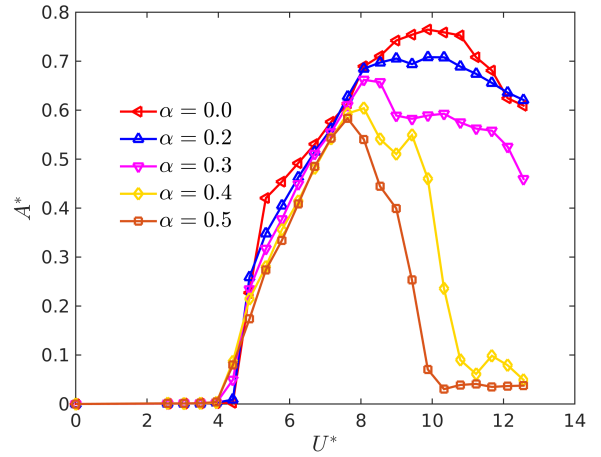


Figure 6: The variation of vibration amplitude response with the reduced velocity for different α .

characterising the flow past rotating bluff bodies. It is defined as $\alpha = D\omega/2U$, where ω is the rotation rate of the sphere in radians per second. It signifies how fast the surface of the sphere is spinning relative to the incoming flow velocity. For investigating the effect of α on the vibration response of the sphere, U^* was varied from 3 to 14 in increments of 0.5. The response was studied for 5 rotation ratios $\alpha = 0.0, 0.2, 0.3, 0.4$ and 0.5 . For this set of experiments, the mass ratio of the system was 14, the natural frequency in water was 0.28Hz , and the damping ratio was 0.0059 .

In figure 6, we see a classic VIV response for $\alpha = 0$, when the sphere is not rotating. When α is gradually increased from 0 to 0.3, the response shape looks similar to the non-rotating case, but the amplitude of vibration decreases. For $\alpha \geq 0.4$, we see a drastic drop in the response. For all these cases, the amplitude suddenly drops after reaching the maximum amplitude of oscillations. As the α is increased, the synchronisation region (parameter space for which the resonance is observed) becomes narrower. The magnitude of peak oscillation also decreases consistently with the rotation up to $\alpha = 0.5$.

The peak amplitude occurs for a smaller U^* with increasing α .

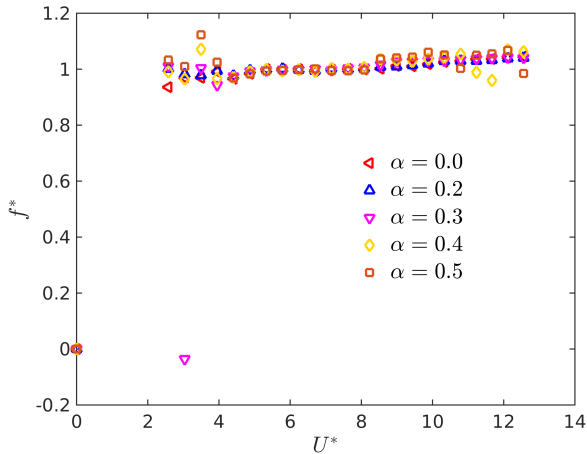


Figure 7: The variation of the non-dimensional frequency of oscillation of the sphere with the reduced velocity for different α .

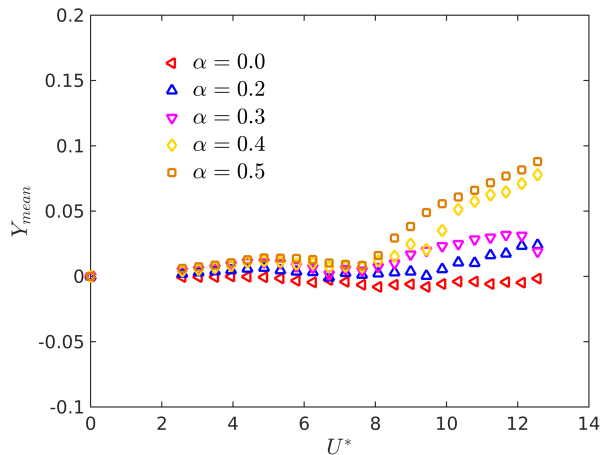


Figure 8: The variation of mean displacement of the sphere with the reduced velocity for different α .

The dominant frequency of oscillations stayed close to the natural frequency of the system for all the α values as shown in figure 7. This indicates that the rotation does not completely suppress the vortex shedding and the sphere remains locked-in for all the cases.

Figure 8 shows how the mean displacement of the sphere varies with increasing rotation. The mean displacement initially is zero for the non-rotating case but increases with the α , which is an effect of the Magnus force acting on the sphere in the direction of rotation. Vorticity measurements by [2] showed planar symmetric vortex loops emanating from the two sides of a non-rotating sphere undergoing VIV. The transverse rotation imposes asymmetry in the flow, causing the loops to bend towards one side due to the Magnus effect, which in consequence increases the ‘lift force’ in the direction of rotation. In the case of cylinders, some novel asymmetric wake patterns were observed with the transverse rotation, which led to an increase in the oscillation amplitude up to 1.9 times the diameter [1]. However, the flow past a sphere is three-dimensional and complex. How the transverse rotation changes the wake patterns and the forces experienced by the sphere, is currently under investigation.

Conclusions

A series of experiments was performed to investigate the effect of transverse rotation on the VIV response of an elastically mounted sphere in terms of amplitude and frequency response. The amplitude of oscillations was lowered with increasing rotation. The synchronisation regime became narrower and the peak response occurred at a lower U^* compared to the non-rotating case. The frequency of oscillation remained close to the natural frequency of the system for all the cases.

Acknowledgements

AS acknowledges the support of a Monash Graduate Scholarship (MGS) and Monash International Postgraduate Research Scholarship (MIPRS). The research was supported by an Australian Research Council Discovery Project grant (DP150102879).

References

- [1] Bourguet, R. and Lo Jacono, D., Flow-induced vibrations of a rotating cylinder, *J. Fluid Mech.*, **740**, 2014, 342–380.
- [2] Govardhan, R. N. and Williamson, C. H. K., Vortex-induced vibrations of a sphere, *J. Fluid Mech.*, **531**, 2005, 11–47.
- [3] Jauvtis, N., Govardhan, R. and Williamson, C. H. K., Multiple Modes of Vortex-Induced Vibration of a Sphere, *J. Fluids Struct.*, **15**, 2001, 555–563.
- [4] Kim, D., Laminar flow past a sphere rotating in the transverse direction, *J. Mech. Sci. Technol.*, **23**, 2009, 578–589.
- [5] Mirauda, D., Volpe Plantamura, a. and Malavasi, S., Dynamic Response of a Sphere Immersed in a Shallow Water Flow, *J. Offshore Mech. Arct. Eng.*, **136**, 2014, 021101.
- [6] Parkinson, G., Phenomena and modelling of flow-induced vibrations of bluff bodies, *Prog. Aerosp. Sci.*, **26**, 1989, 169–224.
- [7] Poon, E. K. W., Ooi, A. S. H., Giacobello, M., Iaccarino, G. and Chung, D., Flow past a transversely rotating sphere at Reynolds numbers above the laminar regime, *J. Fluid Mech. Fluid Mech. J. Mech. Sci. Technol.*, **759**, 2014, 751–781.
- [8] Sarpkaya, T., Vortex-Induced Oscillations, *J. Appl. Mech.*, **46**, 1979, 241–258.
- [9] Zhao, J., *Flow-Induced Vibration of Circular and Square Cylinders with Low Mass and Damping*, Ph.D. thesis, Monash University, 2012.